NATIONAL ADVISORY COMMITTEE FOR AERONAUTICS

WARTIME REPORT

ORIGINALLY ISSUED
May 1944 as
Advance Restricted Report L4E25

INVESTIGATION OF EFFECT OF SIDESLIP ON LATERAL STABILITY CHARACTERISTICS I - CIRCULAR FUSELAGE WITH VARIATIONS IN VERTICAL-TAIL AREA AND TAIL LENGTH WITH AND WITHOUT HORIZONTAL TAIL SURFACE

By Leo F. Fehlner and Robert MacLachlan

Langley Memorial Aeronautical Laboratory
Langley Field, Va.

WASHINGTON

NATIONAL ADVISORY COMMITTEE FOR AERONAUTICS

ADVANCE RESTRICTED REPORT

INVESTIGATION OF EFFECT OF SIDESLIP ON LATERAL STABILITY CHARACTERISTICS I - CIRCULAR FUSELAGE WITH VARIATIONS IN VERTICAL-TAIL AREA AND TAIL LENGTH WITH AND WITHOUT HORIZONTAL TAIL SURFACE

By Leo F. Fehlner and Robert MacLachlan

SUMMARY

The results of tests of a circular fuselage with various combinations of tail lengths and vertical tail surfaces with and without the horizontal tail surface in the 6- by 6-foot test section of the NACA stability tunnel are reported in the form of diagrams of variation of coefficients of lateral force and yawing moment with angle of yaw and angle of attack.

The results of these tests indicated that the change in the unstable yawing moment of the fuselage alone due to increased tail length did not appreciably affect the yawing moment of a fuselage and vertical-tail combination. The addition of a horizontal tail increased the efficiency of the vertical tail in normal-flight attitudes and in the region of negative angles of attack. Existing methods of computing tail effectiveness gave results within ±7 percent of the measured values for the cases computed.

INTRODUCTION

Desirable qualities for the lateral stability and control characteristics of an airplane are dependent on the set of stability derivatives peculiar to the airplane. The stability derivatives can be changed by changes in airplane parameters, such as vertical-tail area, horizontal-tail area, and tail length.

Extensive tests to determine the changes in stability derivatives effected by uniform changes in airplane parameters have been made with a model geometrically similar to the model used in the present investigation. Included in these tests were the effects of cowlings, of wing positions, and of the presence of a vertical tail (references 1 and 2). Reference 1 is mainly concerned with lift and drag characteristics, whereas reference 2 deals with the effects of yaw on the lateral stability characteristics of a rectangular wing with a circular fuselage and vertical tail.

The present investigation, in which the model was tested without wings, is an attempt to determine experimentally the basic changes in stability derivatives caused by uniform changes in vertical-tail area and tail length and by the presence of a horizontal tail. Because a geometrically similar model has been tested in the LMAL 7- by 10-foot tunnel (reference 3), the data may be used for correlating the results in the two wind tunnels.

The tests were made in the NACA stability tunnel and included an angle-of-attack range from -10° to 20° and an angle-of-yaw range from 12° to -30° with various combinations of three fuselages of different lengths and five vertical-tail areas with and without a horizontal tail surface. Two combinations of the model parts used in the present tests are geometrically similar to the model used in the LMAL 7- by 10-foot tunnel for the tests of references 2 and 3.

APPARATUS AND MODEL

The tests were made in the NACA stability tunnel 6- by 6-foot closed-throat test section with the regular six-component balance.

The principal dimensions and the arrangement of the parts of the model used in the investigation are shown in figure 1. All the model parts are made of laminated mahogany. Figure 2 shows the model unassembled, and figure 3 shows the model mounted on the model support. The horizontal strut supporting the model does not rotate in pitch with the model. The vertical struts rotate in yaw with the model and remain alined with the relative wind.

The fuselage is of circular cross section. Its length can be changed by the use of three interchangeable tail cones. When the shortest of these tail cones is attached, the fuselage is geometrically similar to the circular fuselage described in reference 1 and to the model used for the tests reported in reference 2. The coordinates for the medium and long tail cones were obtained by extending the abscissa for the length of the short tail cone according to the formula

$$X_1 = X_o + X_o(c - 1) \sin \frac{\pi}{2a} X_o$$

where

X_o abscissa for original length

a length of portion to be distorted

c ratio of original length of portion to be distorted to final length of portion distorted

X_1 abscissa for final length of distorted portion

The ordinates corresponding to X_1 are taken as those corresponding to X_o from which X_1 was computed. The tail lengths, the lengths of the three fuselages and tail cones, and the ratios of the tail lengths to the 48-inch span of the proposed wing are given in table 1.

Five geometrically similar vertical tail surfaces were made to conform to the NACA 0009 section. In plan form they are representative of the vertical tail surfaces used on the average airplane. The geometric aspect ratio of each vertical tail is 2.15. The horizontal tail surface was made to conform to the NACA 0009 section. Its geometric aspect ratio is 3.99. The numbers by which the tail surfaces are designated, their areas, and the ratios of these areas to a proposed rectangular wing area of 361 square inches are given in table 2.

TESTS

The model combinations tested are given in table 3.

Angle-of-attack tests for each model combination were made over a range from -10° to 20° at angles of yaw

of -5°, 0°, and 5°. Angle-of-yaw tests for each model combination were made over a range from 12° to -30° at angles of attack of -10°, 0°, 10°, and 20°.

The dynamic pressure for the tests was 65 pounds per square foot, which corresponds to a velocity of about 160 miles per hour. The Reynolds number based on an 8-inch wing chord was about 888,000.

RESULTS

The results are presented as standard nondimensional coefficients based on the dimensions of a rectangular wing proposed for the model. The following symbols are used herein and the senses are defined relative to a person within the airplane facing the direction of motion:

C_Y lateral-force coefficient (Y/qS_w)

C_n yawing-moment coefficient (N/qS_wb)

Y lateral force (positive to right)

N yawing moment (positive when right wing tip tends to move rearward)

q dynamic pressure $\left(\frac{1}{2}\rho V^2\right)$

ρ air density

V tunnel-air velocity

$C_{Y_\psi} = \frac{\partial C_Y}{\partial \psi}$

$C_{n_\psi} = \frac{\partial C_n}{\partial \psi}$

ψ angle of yaw, degrees (positive when right wing tip has moved rearward)

α angle of attack, degrees (positive when tail has been depressed)

l tail length

b wing span (48 in.)

S_f vertical-tail area

S_s horizontal-tail area

S_w wing area (361 sq in.)

A_f aspect ratio of vertical tail surface

Figure 4 shows the system of axes used in the measurement of forces, moments, and angles. The axes are fixed in the model for all changes in angle of yaw. For changes in angle of attack, the X-axis remains in the plane in which it was located at $\alpha = 0^\circ$. The axes intersect the model at the assumed center of gravity, which is 10.40 inches behind the nose.

The lateral-stability derivatives are computed, for the range of angle of attack, from measurements of lateral force and yawing moment at angles of yaw of $\pm 5^\circ$; the variation of the forces and moments with angle of yaw is assumed to be linear over the $\pm 5^\circ$ range of angle of yaw.

Angle-of-yaw tests were made to check the linearity of the curves of C_Y and C_n against angle of yaw in the $\pm 5^\circ$ angle-of-yaw range. The slope of these curves shows that the variation of the forces and moments within the angle-of-yaw range of $\pm 5^\circ$ is linear except at high angles of attack. The measured slopes of these curves are plotted with tailed symbols in the figures.

The measurements of lateral-force coefficient C_Y are considered accurate to ± 0.0012 and of yawing-moment coefficient C_n to ± 0.0005. The angle-of-yaw measurements are accurate to about 0.05°, and the angle of attack is accurate to about 0.1°.

A model geometrically similar to the NACA stability tunnel model was tested in the LMAL 7- by 10-foot tunnel and the results of the tests were reported in reference 3. The model consisted of the short fuselage, vertical tail surface 4, and the horizontal tail surface and was tested in the LMAL 7- by 10-foot tunnel at a dynamic pressure of 16.37 pounds per square foot, which corresponds to a velocity of 80 miles per hour. The Reynolds number based on a 10-inch chord was 619,000 and the turbulence factor was 1.6. The model tested in the NACA stability tunnel is eight-tenths the size of the model tested in the LMAL 7- by 10-foot tunnel and was

tested at a dynamic pressure of 65 pounds per square foot corresponding to a velocity of 160 miles per hour and a Reynolds number of 888,000. The turbulence of the air stream in the NACA stability tunnel is not known but is believed to be lower than that of the LMAL 7- by 10-foot tunnel. Variation of C_{Y_ψ} and C_{n_ψ} with α for the similar models are shown in figure 5. Values of C_{Y_ψ} and C_{n_ψ} agree well for the two sets of data. The maximum discrepancies occur at high angles of attack in the region of the stall.

In order to check the data obtained in the NACA stability tunnel, a temporary one-component spring balance was installed to measure the yawing moment due to sideslip. The model support consisted of a cylindrical rod fixed perpendicular to the top of the tunnel by a tripodal wire stay. The model was supported in the same position in the tunnel as on the regular tunnel balance except that it was inverted. Such an arrangement was expected to give altogether different interference effects from the regular support. Figure 6 shows the variation of C_n with ψ thus obtained for a typical case at an angle of attack of 0° and compared with similar data for the model on the regular support in the NACA stability tunnel and in the LMAL 7- by 10-foot tunnel. The two sets of data obtained in the NACA stability tunnel check each other. The data obtained from the LMAL 7- by 10-foot tunnel check the slope from the NACA stability tunnel within 8 percent. This difference in slope is the same as the difference shown in figure 5 for C_{n_ψ} at an angle of attack of 0°. The source of the discrepancy is not obvious from the data but may be the differences in the deflection of the models, angularities of the air stream, or model-size to jet-size ratios.

The results are presented in the form of curves that show the effects of changes in fuselage length for fuselage alone in figures 7 and 8; of changes in vertical-tail area, figures 9 and 10; of changes in tail length, figures 11 to 13; of adding the horizontal tail surface, figures 14 to 16; and of changes in tail length and vertical-tail area with constant tail volume, figures 17 and 18. The data plotted in the various figures and the model combinations used in obtaining each plot are summarized in table 4.

DISCUSSION

Effect of Changes in Fuselage Length for Fuselage Alone

The effect of changes in fuselage length on the stability of the fuselage alone is shown in figures 7 and 8. The derivative C_{Y_ψ} was increased by an increment of 0.0007 by increasing the value of l/b from 0.418 to 0.618. The absolute magnitude of this increment is small compared with the magnitude of derivatives for the fuselage with the vertical tail surfaces tested. The derivative C_{n_ψ} is very slightly changed by the change in fuselage length relative to the magnitude of the derivatives for the complete model. Although theoretical analysis indicates that the unstable yawing moment of the fuselage alone varies with fineness ratio and volume, this variation has not been detected herein because the magnitude of the variation is of the same order as that of the experimental accuracy.

Effect of Changes in Vertical-Tail Area

The effect of changes in vertical-tail area (horizontal tail on) is shown in figures 9 and 10. At an angle of yaw of -10° and at an angle of attack of 0°, changing S_f/S_w from a value of 0.0659 to 0.0974 increased C_Y by an increment of 0.019 and C_n by an increment of 0.0097. Throughout the angle-of-attack range, the same change in S_f/S_w increased C_{Y_ψ} by an increment of about 0.0014 and C_{n_ψ} by an increment of about 0.00098.

The values of C_{Y_ψ} and C_{n_ψ} decrease with angle of attack; the decrease for a change in angle of attack from -5° to 5° is 0.00043 for C_{n_ψ} with vertical tail surface 2 and 0.00048 with vertical tail surface 4. The decrease in C_{Y_ψ} for the same decrease in angle of attack and for either vertical-tail area is 0.0012.

Effect of Changes in Tail Length

The effect of changes in tail length is shown in figures 11 to 13 for the model with the horizontal tail surface and vertical tail surface 4. The change in C_Y due to changing l/b from 0.418 to 0.618 is small and probably negligible for cases in which the lateral force is largely the contribution of the vertical tail surface. The effect on C_{Y_ψ} as shown in figure 12 appears inconsistent but is small and therefore probably negligible.

The yawing moment due to sideslip increases with tail length. This increase in C_n increases with ψ up to shortly after the stall of the vertical tail surface. At values of ψ beyond the stall, C_n is increased about 0.01 by an increase in tail length of 0.1.

Changing the value of l/b from 0.418 to 0.518 causes an increase in C_{n_ψ} of approximately 0.0007 throughout the angle-of-attack range. An increase in l/b, however, from 0.518 to 0.618 causes increases of 0.00059 and 0.00046 in C_{n_ψ} at angles of attack of -5° and 5°, respectively. Increasing the angle of attack decreases C_{n_ψ}. For the short, medium, and long tail lengths, the decrease in C_{n_ψ} is 0.00015, 0.00037, and 0.00050, respectively, for an increase in angle of attack from -5° to 5°.

The effect on C_{n_ψ} and C_{Y_ψ} of changing the vertical-tail area and tail length is shown in figure 13. The model, in this case, is at an angle of attack of 2° and is equipped with the horizontal tail surface. Increases in vertical-tail area produce regular increases in both C_{Y_ψ} and C_{n_ψ}. Increases in tail length produce regular increases in C_{n_ψ} except for the extremely small values of S_f/S_W for which the directional instability is of the same order of magnitude as for the fuselage alone. For all practical values of S_f/S_W, therefore, increasing

tail length increases the directional stability as measured by C_{n_ψ}.

Effect of Horizontal Tail Surface

The removal of the horizontal tail surface decreases the efficiency of the vertical tail surface in all attitudes except at large angles of attack. (See figs. 14 to 16.) For the long fuselage, at -5° angle of attack, the value of C_{Y_ψ} is decreased by an increment of 0.001 by removing the horizontal tail surface whereas, at 5° angle of attack, C_{Y_ψ} is not decreased. The effect on C_{Y_ψ}, in general, is the same magnitude for the short-fuselage and vertical-tail combination. For the long fuselage, figure 15 shows a large effect on C_{n_ψ} that varies from a decrease of 0.00090 at an angle of attack of -5° to a decrease of 0.00039 at an angle of attack of 5°. The corresponding decreases for the short-fuselage and vertical-tail combination are 0.00054 and 0.00020. (See fig. 16.) By removing the horizontal tail surface, the efficiency of the vertical tail surface is therefore decreased by an amount that varies with angle of attack. The decrease is slightly greater for the short-fuselage and vertical-tail combination than for the long-fuselage and vertical-tail combination.

Effect of Changes with Constant Tail Volume

The effect of changes in tail length and vertical-tail area with tail volume held constant based on the dimensions given for the model is shown in figures 17 and 18. The derivative C_{Y_ψ} increases as the vertical-tail area increases and as the tail length decreases. The value of the derivative C_{n_ψ} theoretically should not vary with changes in tail length and vertical-tail area if the tail volume is held constant. The variation of C_{n_ψ}, measured experimentally, is small over the range of angle of attack from 4° to 12° but is appreciable at negative and at high positive angles of attack.

Comparison with Theoretical Variations

The experimental results have been compared with theory by means of accepted simple calculations that involve a minimum of anticipation for the desired results. The first of these calculations can be made from the expression of the variation of lateral force with sideslip, which can be written as

$$\left(C_{Y_\psi}\right)_{total} = \left(C_{Y_\psi}\right)_{fuselage} + \left(C_{Y_\psi}\right)_f \qquad (1)$$

where $\left(C_{Y_\psi}\right)_{fuselage}$ is the experimental value obtained in this investigation,

$$\left(C_{Y_\psi}\right)_f = 2\pi \frac{S_f}{S_w} \frac{KA_f}{A_f + 2K} \qquad (2)$$

and f denotes vertical tail surface. The constant K is given in reference 4 as 0.875 for an elliptical spanwise loading. If the spanwise loading of the vertical tail surface is assumed to be elliptical for the purposes of analytical treatment and if the model dimensions are used as previously given, values of C_{Y_ψ} for vertical tail surfaces 2 and 4 are 0.00348 and 0.00515, respectively, according to equation (2). The corresponding experimental values computed from the data according to equation (1) at 0° angle of attack and with a horizontal tail on the long fuselage are 0.0038 and 0.0054. The theoretical relation then underestimates the value of C_{Y_ψ} by 9 percent for vertical tail surface 2 and 5 percent for vertical tail surface 4. Similarly, C_{n_ψ} may be written

$$\left(C_{n_\psi}\right)_f = -\frac{l}{b}\left(C_{Y_\psi}\right)_f \qquad (3)$$

Theoretical values of C_{n_ψ} for vertical tail surfaces 2 and 4 on the long fuselage are -0.00215 and -0.00317, respectively. The corresponding experimental values for the model with the horizontal tail surface are -0.00226 and -0.00330. The theoretical relation then underestimates the value of C_{n_ψ} for combinations with the

long fuselage by 5 percent for vertical tail surface 2 and 4 percent for vertical tail surface 4.

The theoretical values of C_{n_ψ} for vertical tail surface 4 in combination with the medium and short fuselages are -0.00267 and -0.00215, respectively. The corresponding values of -0.00277 and -0.00207 were obtained experimentally for the model with the horizontal tail surface. The theoretical relation then underestimates C_{n_ψ} for the medium tail length and vertical tail surface 4 by 4 percent and overestimates C_{n_ψ} for the short tail length and vertical tail surface 4 by 4 percent. If the value of C_{Y_ψ} computed according to equation (2) is increased by 2 percent, the resulting values of C_{Y_ψ} and C_{n_ψ} are within 7 percent for the cases analyzed. This 2-percent increase in C_{Y_ψ} may account for the influence of the horizontal tail surface, the influence of the fuselage, or any peculiarities of flow. The resulting discrepancies, which amount to ±7 percent, are slightly less than twice the limits of discrepancy shown previously between the data from the NACA stability tunnel and the LMAL 7- by 10-foot tunnel.

CONCLUSIONS

The results of tests in the NACA stability tunnel of a circular fuselage with various combinations of tail lengths and vertical tail surfaces with and without the horizontal tail surfaces indicated the following conclusions:

1. The effect of the change in the unstable yawing moment of the fuselage alone due to increased tail length on the variation of yawing moment with sideslip was negligible.

2. At an angle of attack of 2°, the vertical tail surface in the presence of the horizontal tail surface produced values of lateral-force derivative C_{Y_ψ} and yawing-moment derivative C_{n_ψ} that were within 7 percent of the estimated values.

3. The addition of the horizontal tail surface increased the efficiency of the vertical tail surface. The increase in C_{Y_ψ} varied from 0.001 at an angle of attack of -5° to 0 at an angle of attack of 5°; and the increase in C_{n_ψ} varied from 0.00090 at an angle of attack of -5° to 0.00039 at an angle of attack of 5°.

Langley Memorial Aeronautical Laboratory
National Advisory Committee for Aeronautics
Langley Field, Va.

REFERENCES

1. Jacobs, Eastman N., and Ward, Kenneth E.: Interference of Wing and Fuselage from Tests of 209 Combinations in the N.A.C.A. Variable-Density Tunnel. NACA Rep. No. 540, 1935.

2. Bamber, M. J., and House, R. O.: Wind-Tunnel Investigation of Effect of Yaw on Lateral-Stability Characteristics. II - Rectangular N.A.C.A. 23012 Wing with a Circular Fuselage and a Fin. NACA TN No. 730, 1939.

3. Wallace, Arthur R., and Turner, Thomas R.: Wind-Tunnel Investigation of Effect of Yaw on Lateral-Stability Characteristics. V - Symmetrically Tapered Wing with a Circular Fuselage Having a Horizontal and a Vertical Tail. NACA ARR No. 3F23, 1943.

4. Higgins, George J.: The Prediction of Airfoil Characteristics. NACA Rep. No. 312, 1929.

TABLE 1

FUSELAGE DIMENSIONS

Fuselage	Fuselage length (in.)	Tail-cone length (in.)	Tail length, l' (in.) (1)	$\frac{\text{Tail length}}{\text{Wing span}}$, $\frac{l}{b}$
Short	32.25	9.85	20.07	0.418
Medium	37.05	14.65	24.87	.518
Long	41.85	19.45	29.67	.618

[1]Tail length measured from center of gravity, assumed to be 10.40 in. behind nose of the model, to hinge line of tail surfaces.

NATIONAL ADVISORY
COMMITTEE FOR AERONAUTICS

TABLE 2

AREAS OF VERTICAL AND HORIZONTAL TAIL SURFACES

Tail surface	Designation	Tail area (sq in.)	$\frac{\text{Tail area}}{\text{Wing area}}$
Vertical	1	10.83	0.0300
Do-----	2	23.78	.0659
Do-----	3	28.37	.0786
Do-----	4	35.16	.0974
Do-----	5	46.20	.1278
Horizontal	----------	64.21	.178

TABLE 3

MODEL COMBINATIONS TESTED

Combination	Fuselage	Horizontal tail surface	Vertical tail surface	Combination	Fuselage	Horizontal tail surface	Vertical tail surface
1	Short	Off	Off	12	Medium	On	1
2	--do--	---do---	4	13	---do---	---do---	2
3	Long	---do---	Off	14	---do---	---do---	3
4	--do--	---do---	4	15	---do---	---do---	4
5	Short	On	Off	16	---do---	---do---	5
6	--do--	---do---	1	17	Long	---do---	Off
7	--do--	---do---	2	18	---do---	---do---	1
8	--do--	---do---	3	19	---do---	---do---	2
9	--do--	---do---	4	20	---do---	---do---	3
10	--do--	---do---	5	21	---do---	---do---	4
11	Medium	---do---	Off	22	---do---	---do---	5

NATIONAL ADVISORY
COMMITTEE FOR AERONAUTICS

| | | |

TABLE 4

PRESENTATION OF RESULTS

Plot	Model combination	Figure
C_{Y_ψ} and C_{n_ψ} against α	9	[a]5
C_n against ψ	9	[a]6
C_Y and C_n against ψ	1 and 3	7
C_{Y_ψ} and C_{n_ψ} against α	1 and 3	8
C_Y and C_n against ψ	19 and 21	9
C_{Y_ψ} and C_{n_ψ} against α	19 and 21	10
C_Y and C_n against ψ	9,15, and 21	11
C_{Y_ψ} and C_{n_ψ} against α	9,15, and 21	12
C_{Y_ψ} and C_{n_ψ} against $\frac{S_f}{S_w}$ at $\alpha = 2^\circ$	5 to 22	13
C_Y and C_n against ψ	4 and 21	14
C_{Y_ψ} and C_{n_ψ} against α	4 and 21	15
C_{Y_ψ} and C_{n_ψ} against α	2 and 9	16
C_Y and C_n against ψ	9,14, and 19	17
C_{Y_ψ} and C_{n_ψ} against α	9,14, and 19	18

[a]Also shown in this figure are results from LMAL 7- by 10-foot tunnel for model with dimensions geometrically similar to model combination 9 tested in NACA stability tunnel.

NATIONAL ADVISORY
COMMITTEE FOR AERONAUTICS

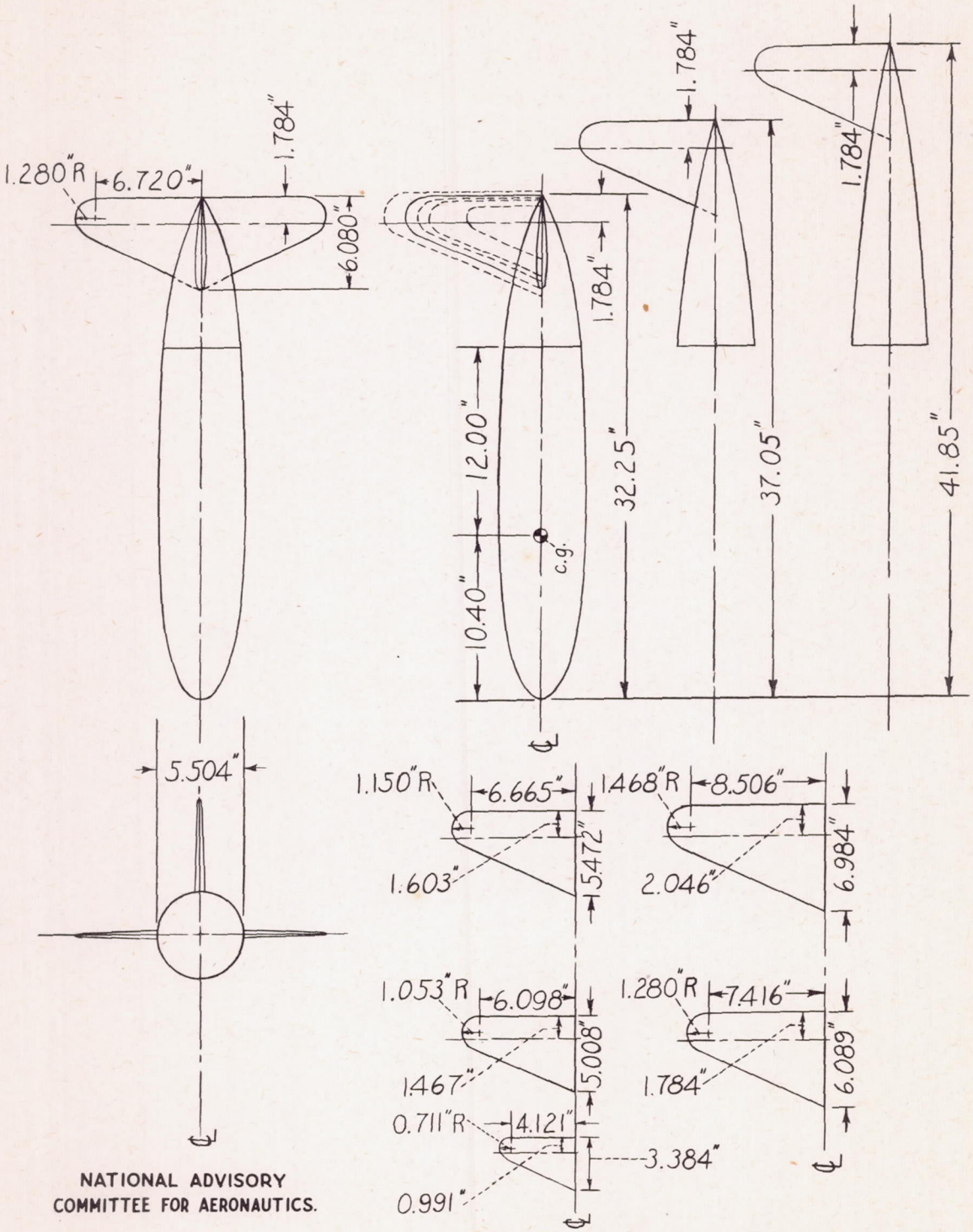

Figure 1.- The circular fuselage, vertical and horizontal tails, and tail cones with the principal dimensions for assembly.

Figure 2.- Parts of model.

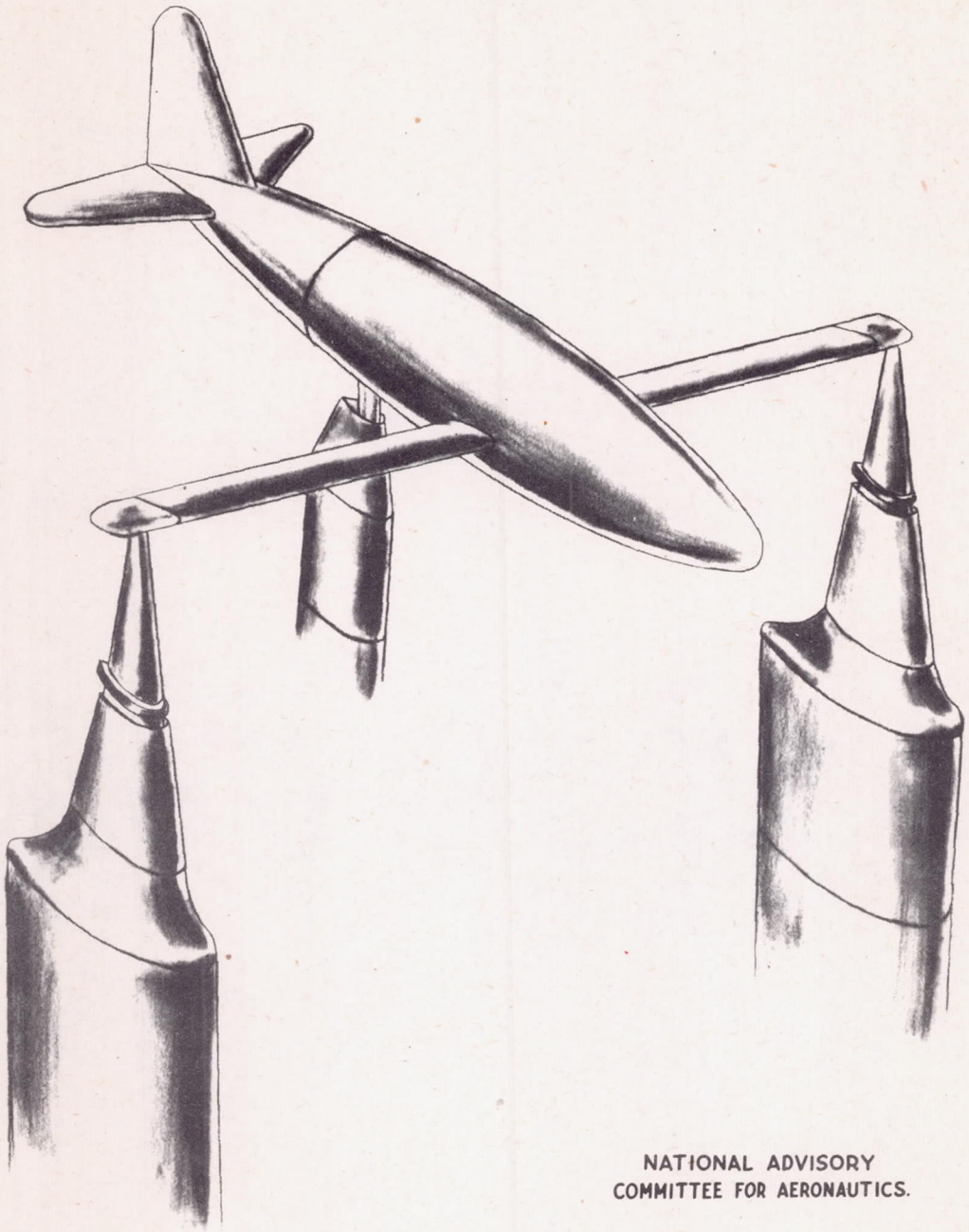

Figure 3.- Model mounted on model support.

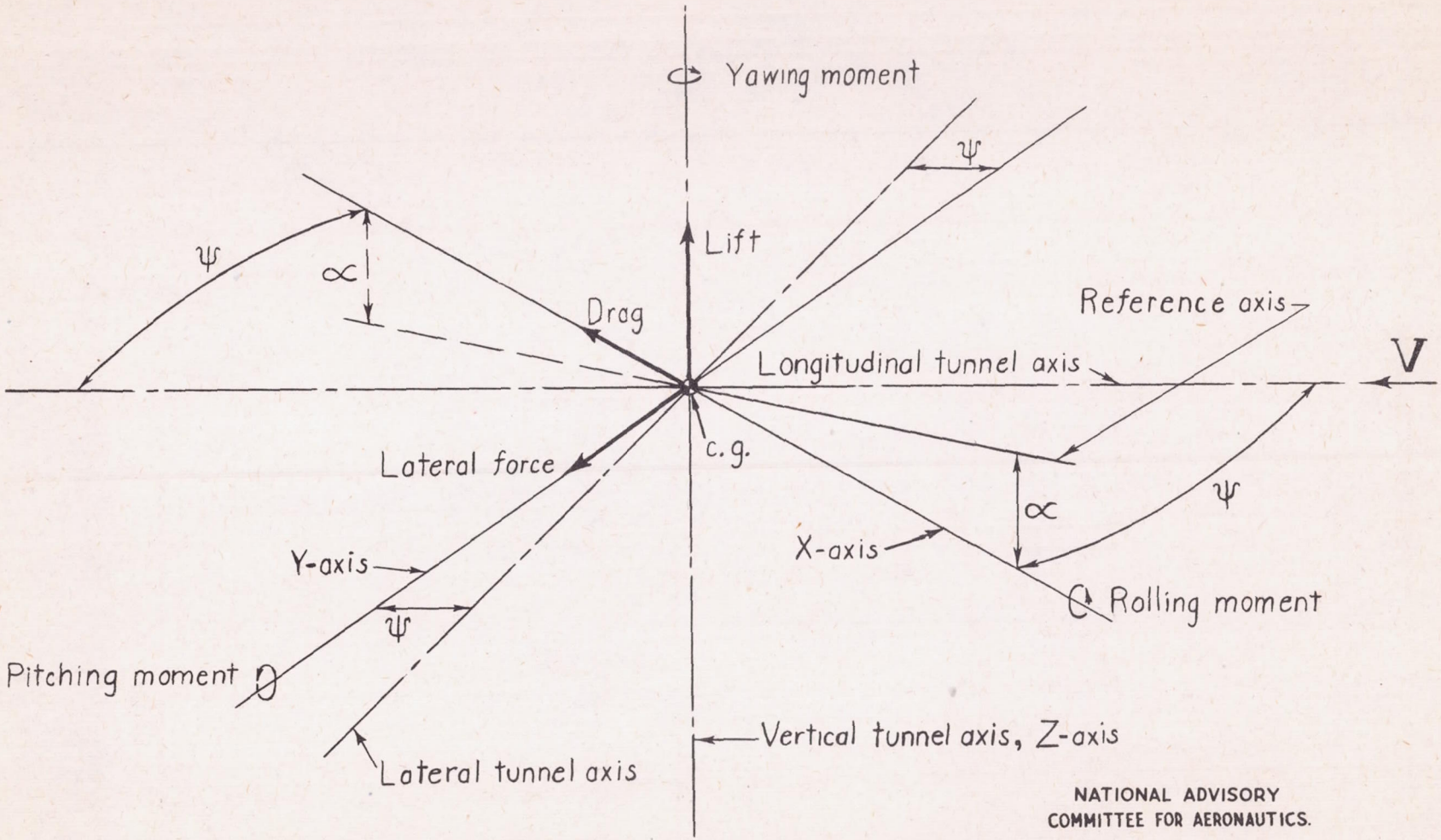

Figure 4.— System of axes used in the measurement of forces, moments, and angles.

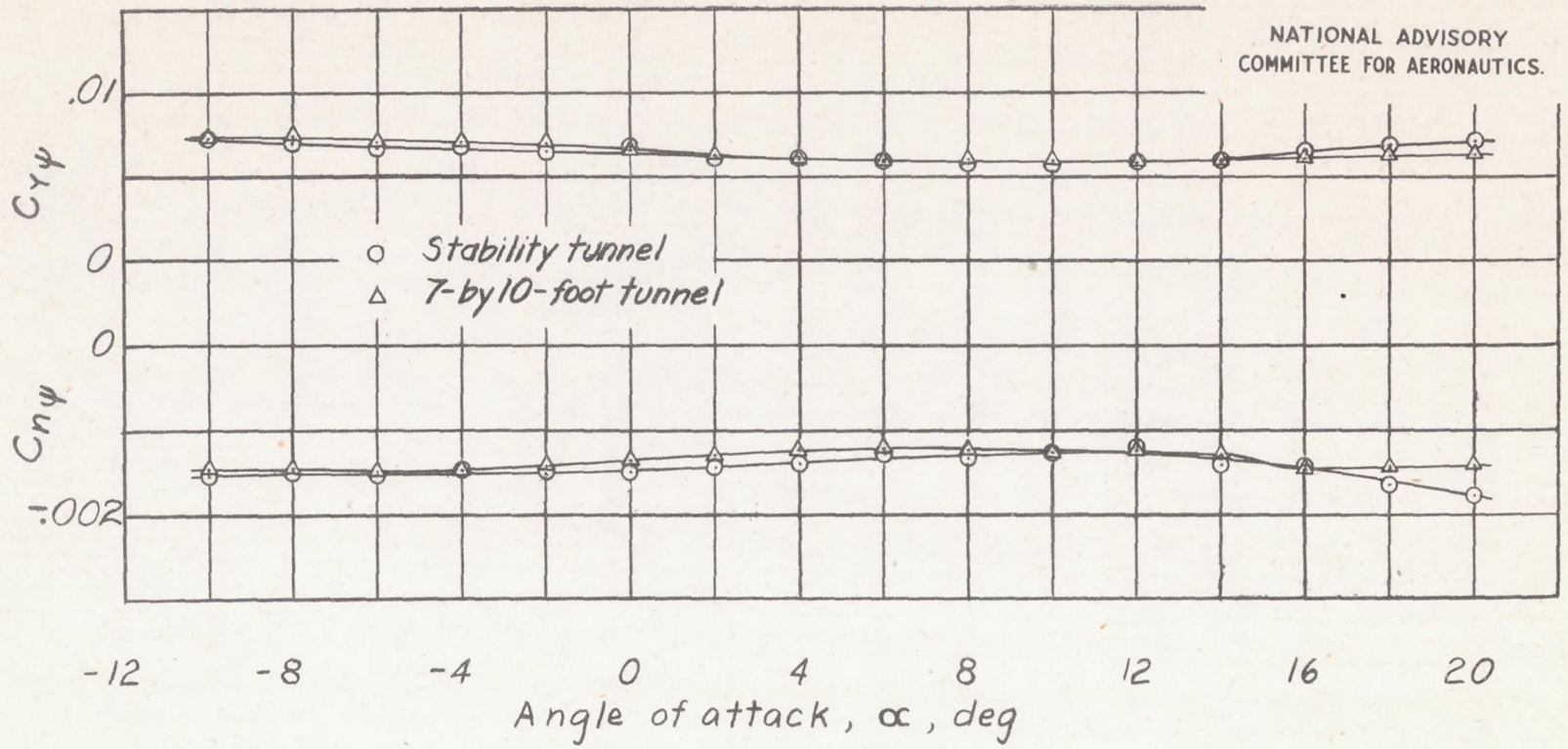

Figure 5.- Comparison of data from NACA stability tunnel and LMAL 7- by 10-foot tunnel for rate of change of stability derivatives C_{Y_ψ} and C_{n_ψ} with angle of attack. Horizontal tail surface on; $\frac{l}{b} = 0.418$; vertical tail surface 4, $\frac{S_f}{S_w} = 0.0974$.

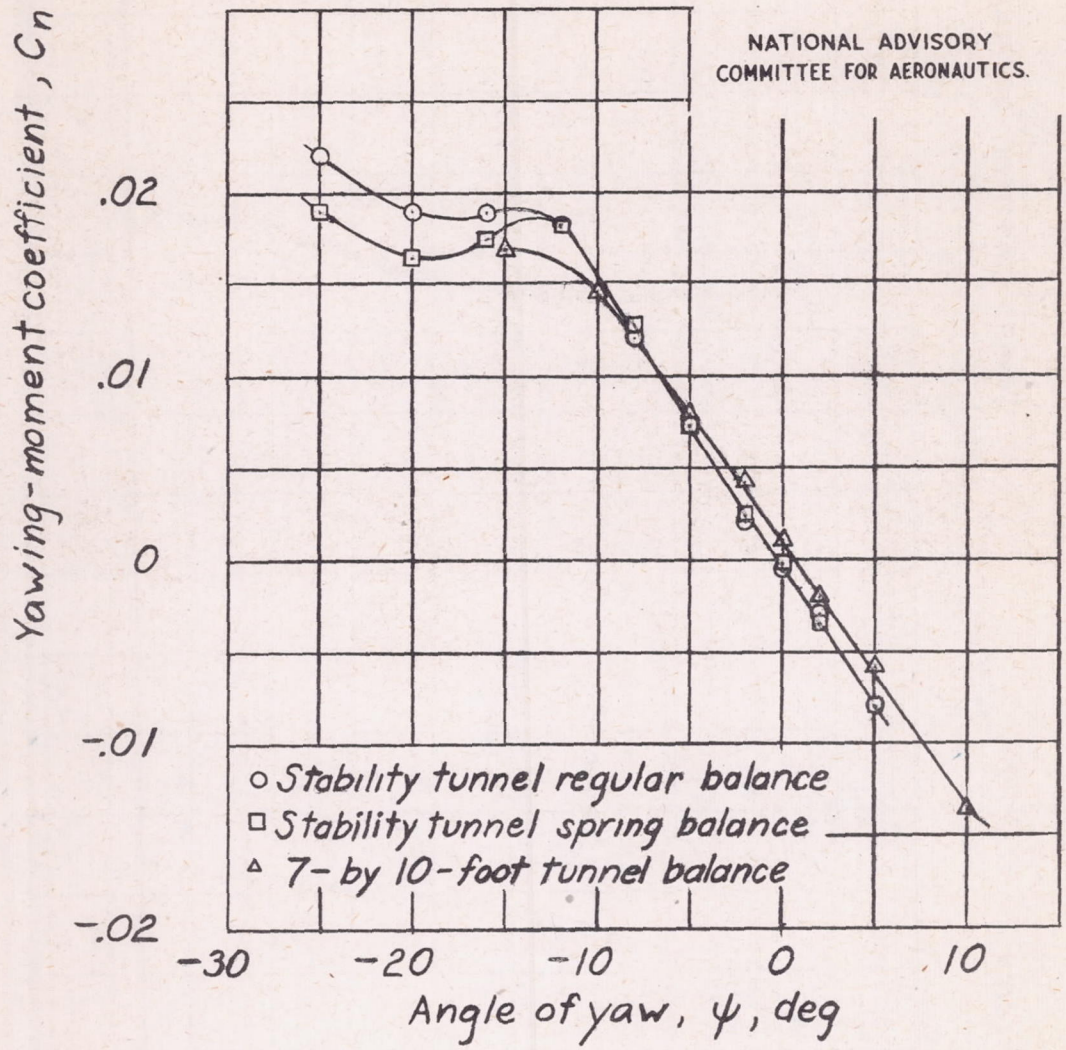

Figure 6.- Comparison of data obtained with NACA stability tunnel regular balance, NACA stability tunnel spring balance, and LMAL 7- by 10-foot tunnel balance for rate of change of yawing-moment coefficient with angle of yaw. Horizontal tail surface on; $\frac{l}{b} = 0.418$; vertical tail surface 4, $\frac{S_f}{S_w} = 0.0974$; $\alpha = 0^\circ$.

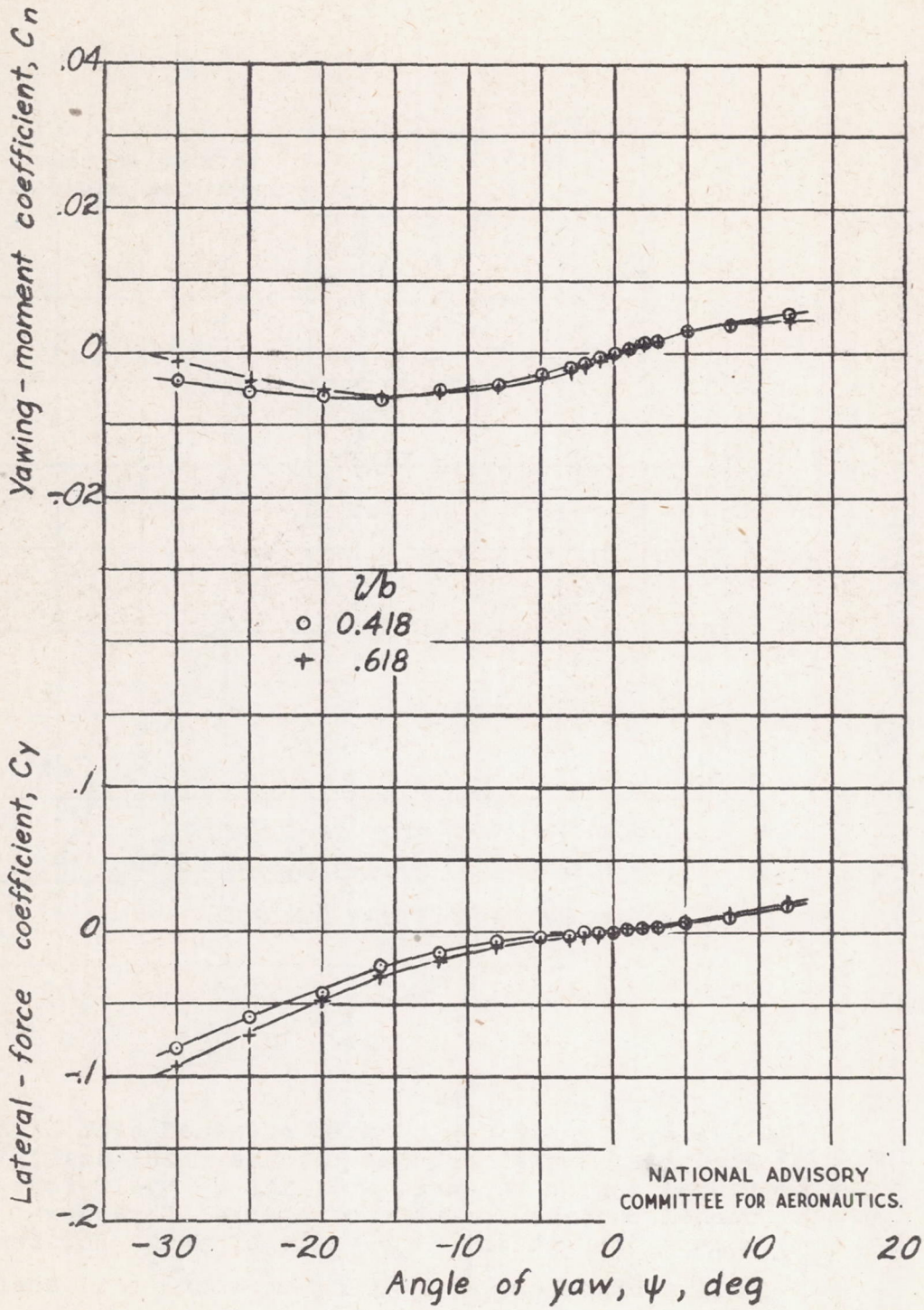

Figure 7.- Effect of changing fuselage length on rate of change of lateral-force and yawing-moment coefficients with angle of yaw. No horizontal or vertical tail surfaces; $\alpha = 0^{\circ}$.

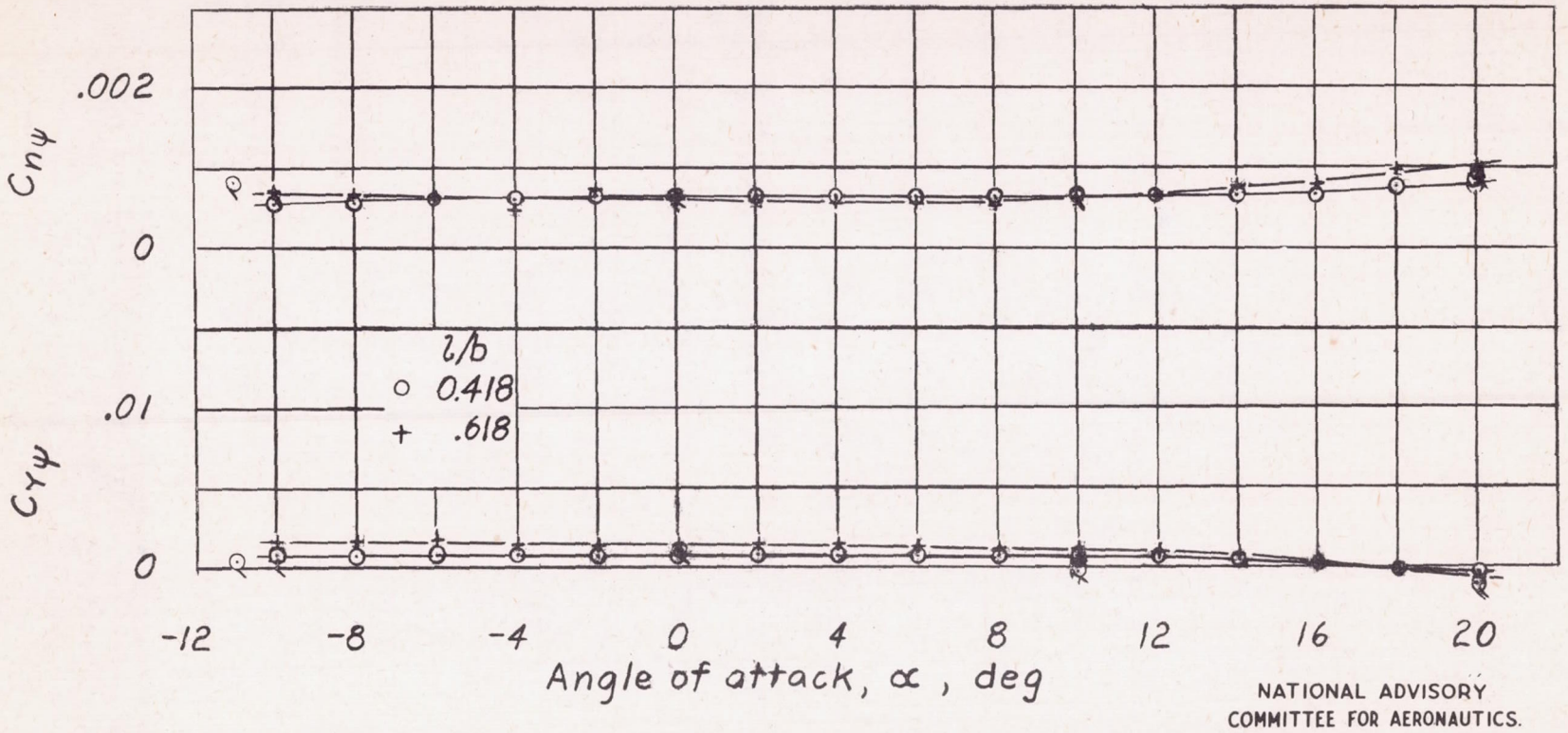

Figure 8.- Effect of changing fuselage length on rate of change of stability derivatives C_{Y_ψ} and C_{n_ψ} with angle of attack.
No horizontal or vertical tail surfaces.

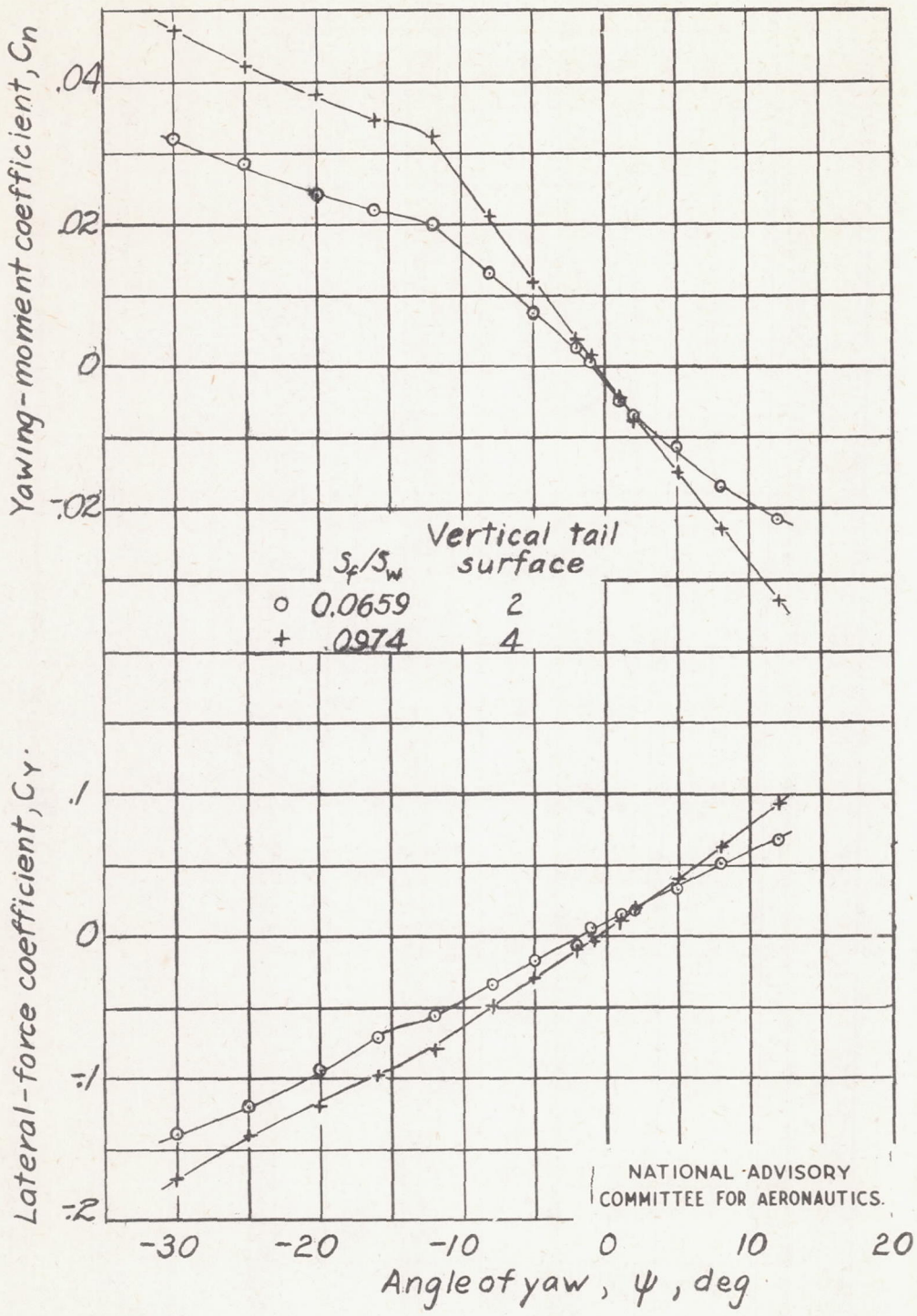

Figure 9.- Effect of changing vertical-tail area on rate of change of lateral-force and yawing-moment coefficients with angle of yaw. Horizontal tail surface on; $\frac{l}{b} = 0.618$; $\alpha = 0^\circ$.

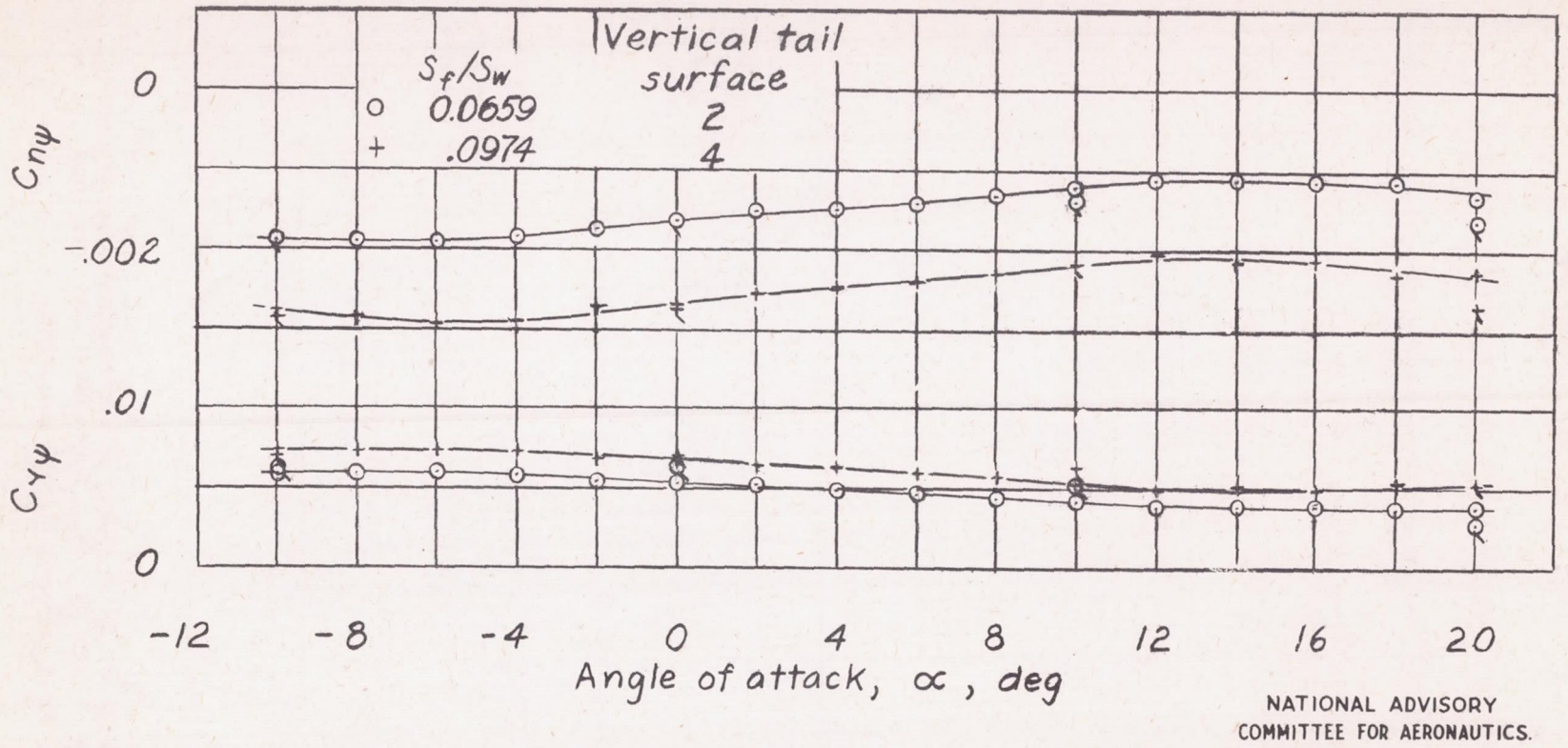

Figure 10.- Effect of changing vertical-tail area on rate of change of stability derivatives C_{Y_ψ} and C_{n_ψ} with angle of attack. Horizontal tail surface on; $\frac{l}{b} = 0.618$.

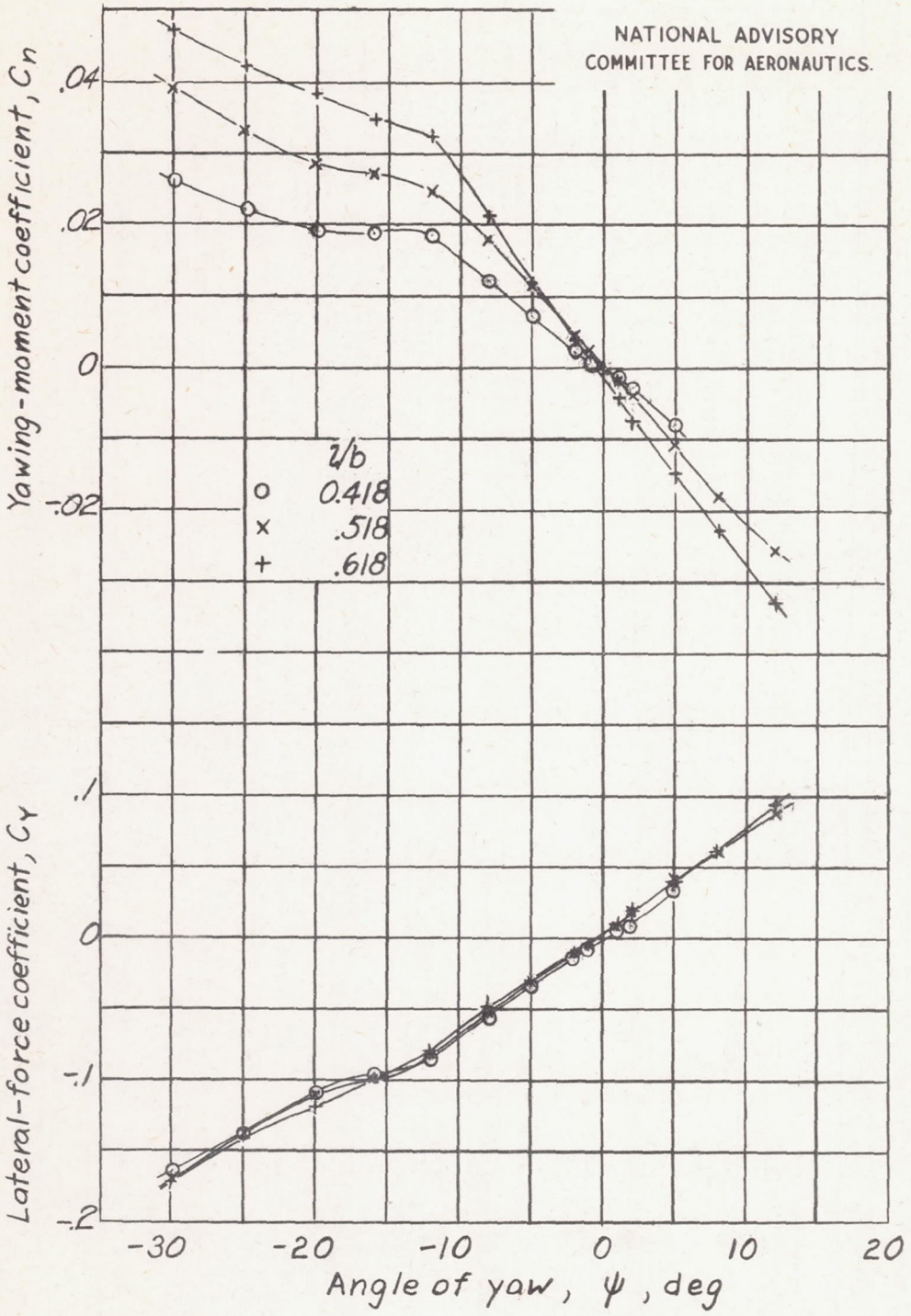

Figure 11.- Effect of changing tail length on rate of change of lateral-force and yawing-moment coefficients with angle of yaw. Horizontal tail surface on; vertical tail surface 4, $\frac{S_f}{S_w} = 0.0974$; $\alpha = 0^\circ$.

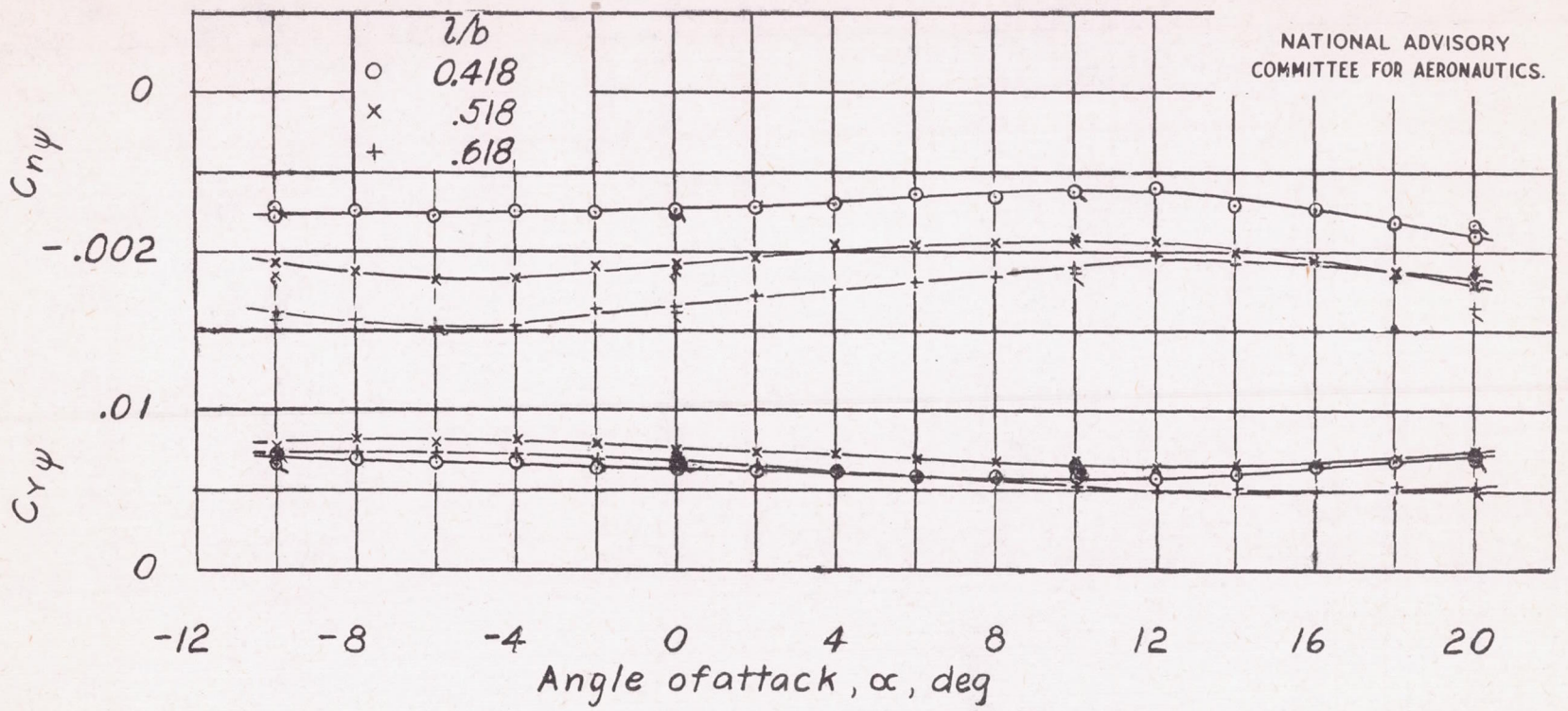

Figure 12.- Effect of changing tail length on rate of change of stability derivatives C_{Y_ψ} and C_{n_ψ} with angle of attack.
Horizontal tail surface on; vertical tail surface 4, $\frac{S_f}{S_w} = 0.0974$.

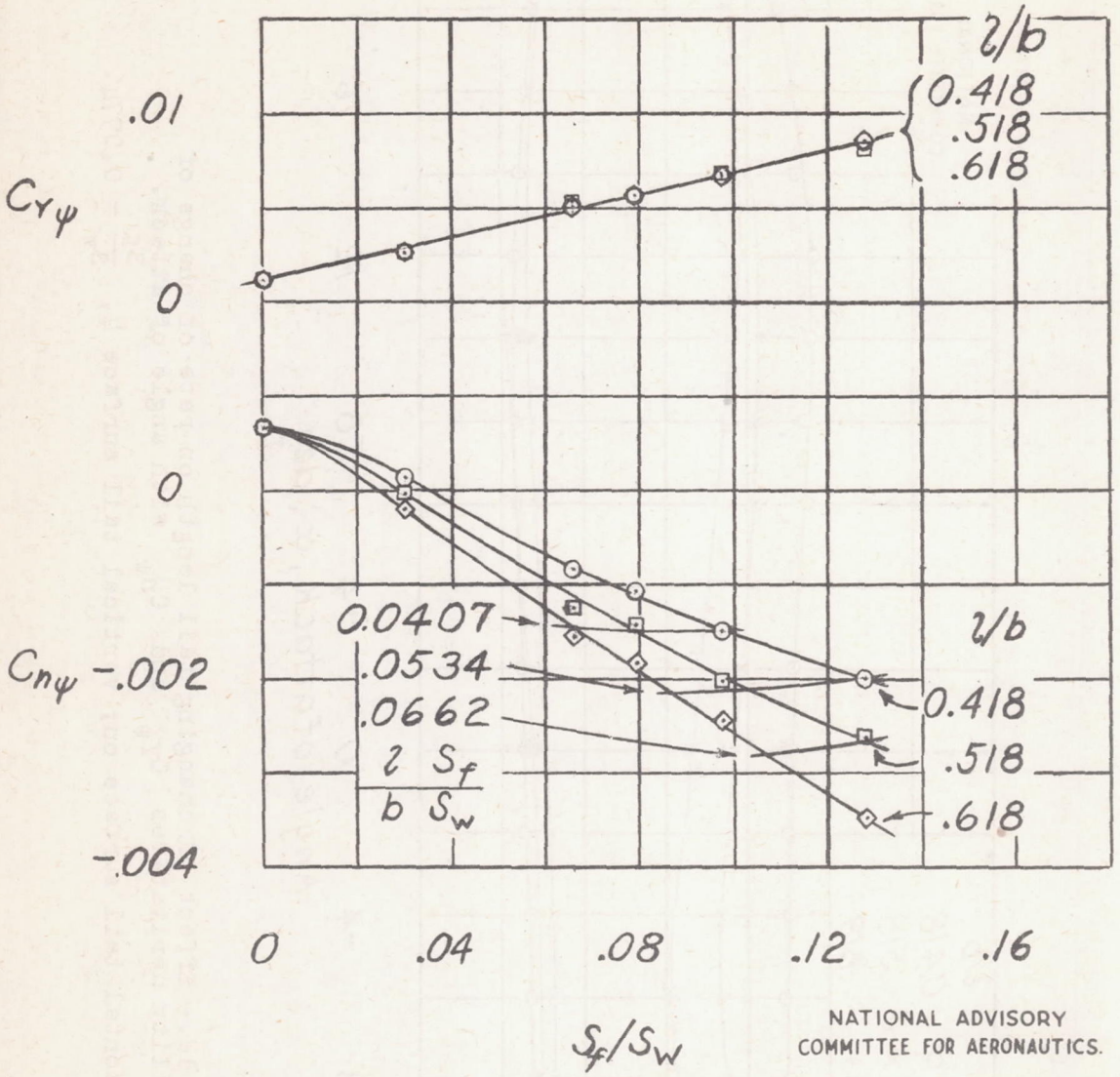

Figure 13.- Effect of changing tail length on rate of change of stability derivatives C_{Y_ψ} and C_{n_ψ} with vertical-tail area. Horizontal tail surface on; $\alpha = 2^\circ$.

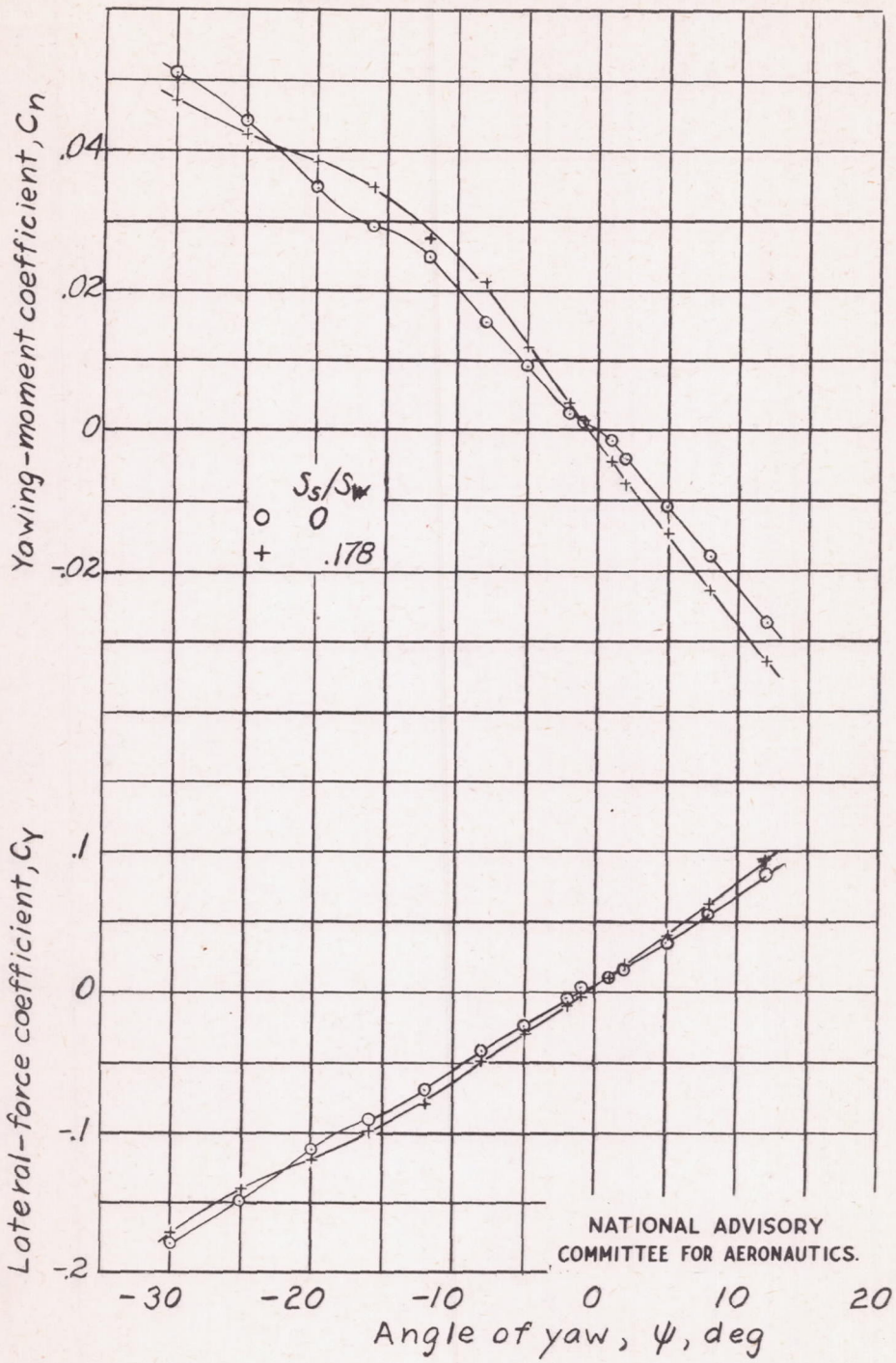

Figure 14.- Effect of horizontal tail surface on rate of change of lateral-force and yawing-moment coefficients with angle of yaw. $\frac{l}{b} = 0.618$; vertical tail surface 4, $\frac{S_f}{S_w} = 0.0974$; $\alpha = 0°$.

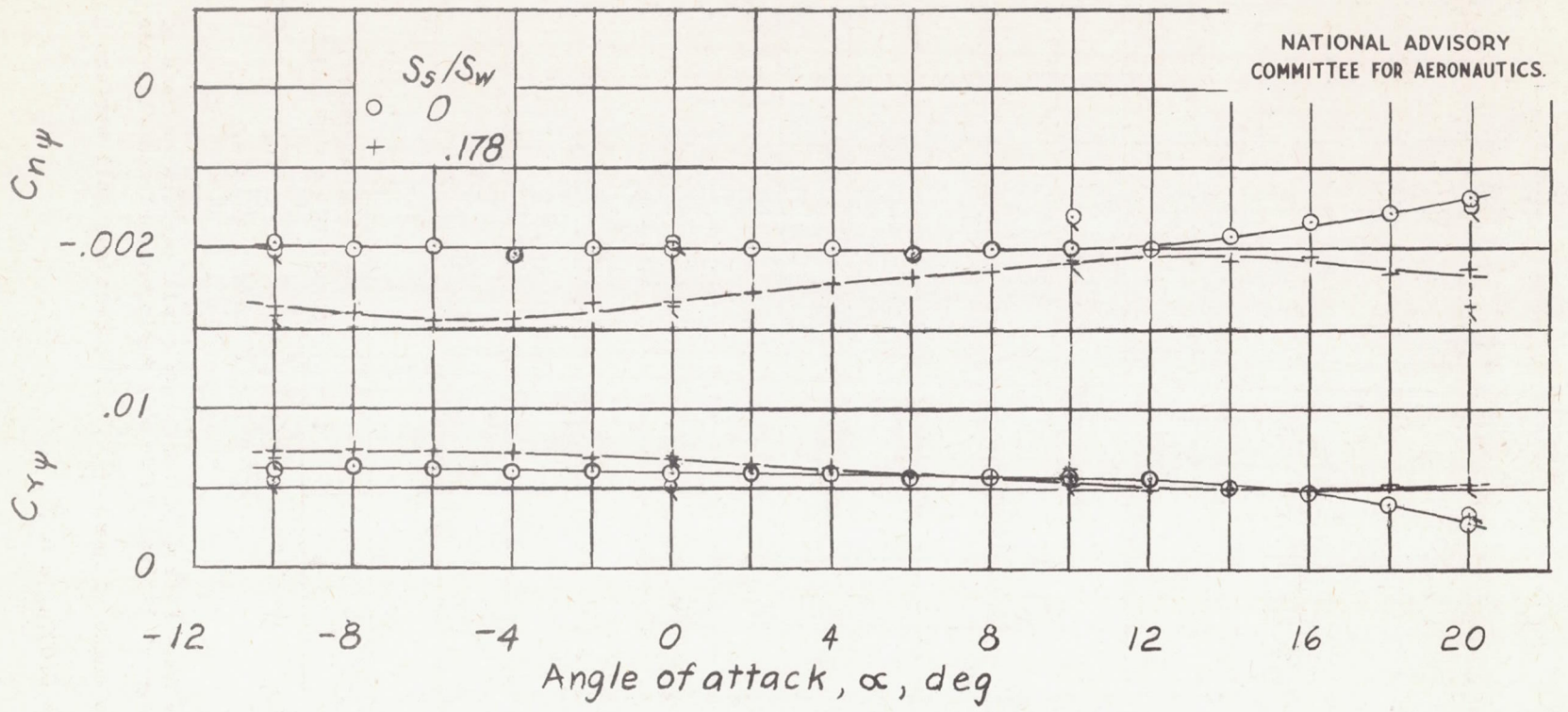

Figure 15.- Effect of horizontal tail surface on rate of change of stability derivatives C_{Y_ψ} and C_{n_ψ} with angle of attack.

$\frac{l}{b} = 0.618$; vertical tail surface 4, $\frac{S_f}{S_w} = 0.0974$.

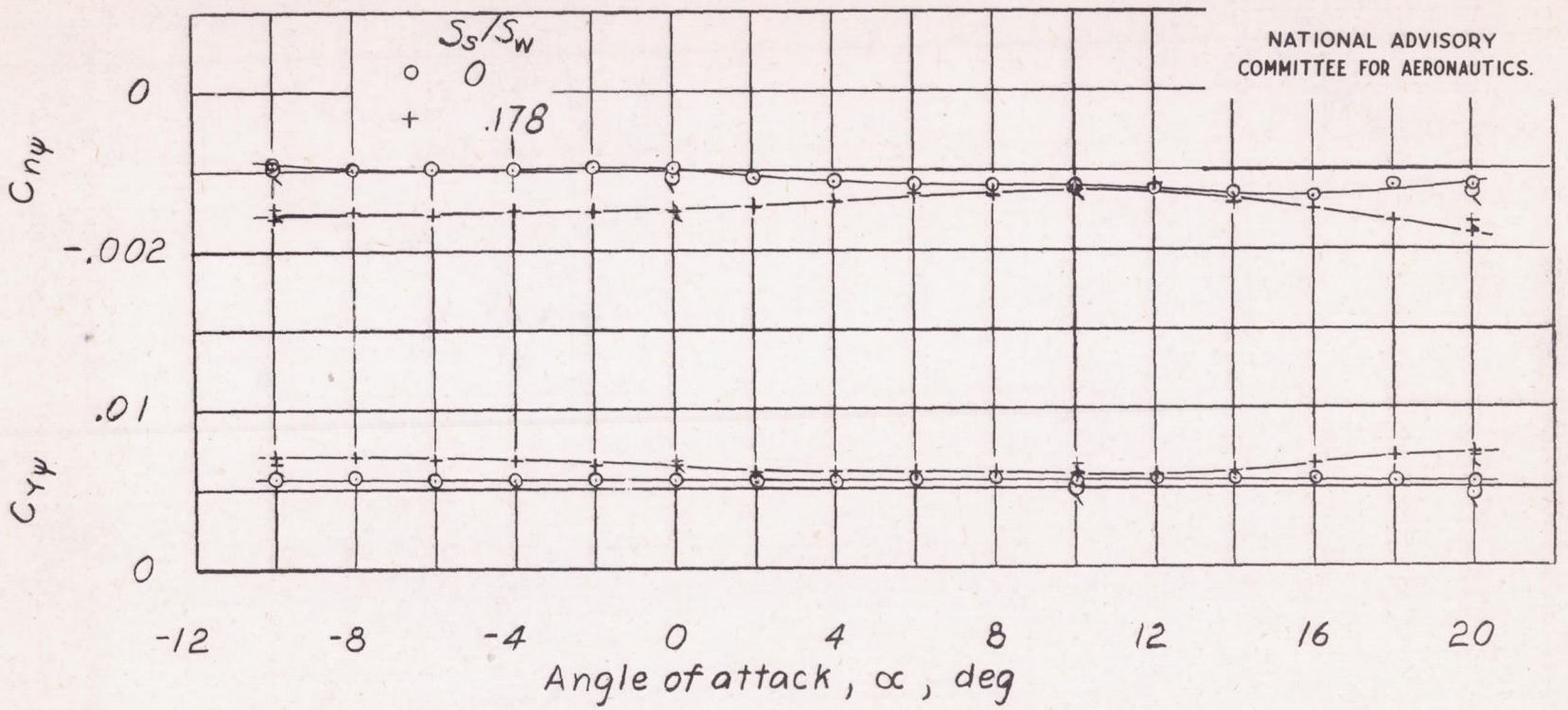

Figure 16.- Effect of horizontal tail surface on rate of change of stability derivatives C_{Y_ψ} and C_{n_ψ} with angle of attack.

$\frac{l}{b} = 0.418$; vertical tail surface 4, $\frac{S_f}{S_w} = 0.0974$.

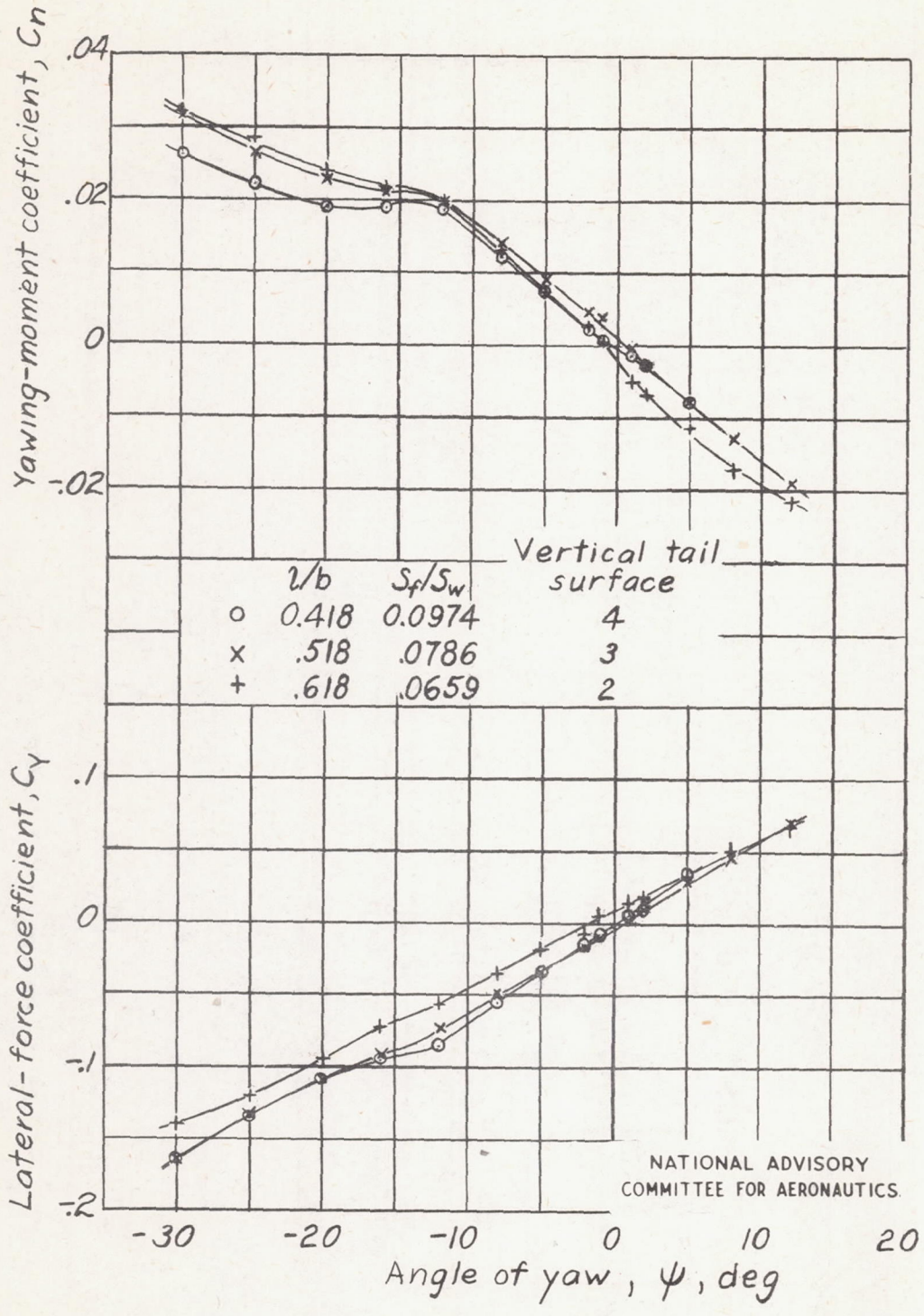

Figure 17.- Effect of different combinations having constant tail volume on rate of change of lateral-force and yawing-moment coefficients with angle of yaw. Horizontal tail surface on; $\alpha = 0^\circ$.

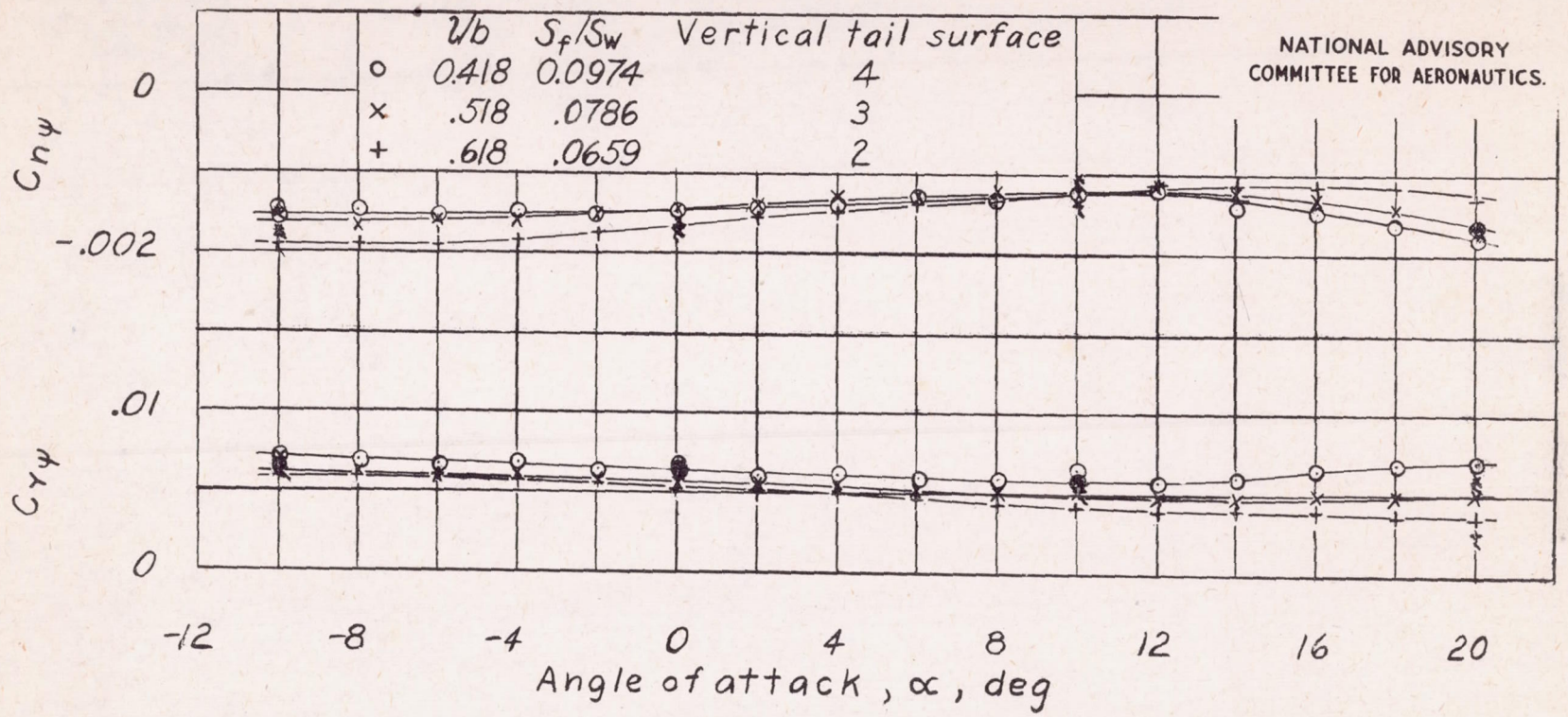

Figure 18.- Effect of different combinations having constant tail volume on rate of change of stability derivatives C_{Y_ψ} and C_{n_ψ} with angle of attack. Horizontal tail surface on.